Terra Nova

doi: 10.1111/ter.12209

Comment

Objective utilization of data from DSDP Site 380 (Black Sea)

Speranta-Maria Popescu,[1] Mihaela Carmen Melinte-Dobrinescu[2] and Jean-Pierre Suc[3]

[1]*GeoBioStratData.Consulting, 385 Route du Mas Rillier, Rillieux la Pape 69140, France;* [2]*National Institute of Marine Geology and Geo-Ecology, 23-25 Dimitrie Onciul Street, Bucharest 70318, Romania;* [3]*Sorbonne Universités, UPMC Université Paris 06, CNRS, Institut des Sciences de la Terre Paris, Paris F-75005, France*

van Baak *et al.* (2015) provide magnetostratigraphy for DSDP Hole 380A along a 175 m interval and a $^{40}Ar/^{39}Ar$ date at 706.8 mbsf. The biostratigraphic basis for their interpretation is the first consistent occurrence (FCO) of the dinoflagellate cysts *Galeacysta etrusca* and *Caspidinium rugosum* at 841 and 850 mbsf respectively (Grothe *et al.*, 2014), instead of at least 1009.36 mbsf as demonstrated by Suc *et al.* (2015) (Fig. 1A). Grothe *et al.* (2014) proposed an age of 6.1 Ma for this event from the Taman Peninsula. We repeat that the placement of this bioevent at 6.1 Ma is significantly lower in the sedimentary succession of Site 380 (Fig. 1A).

van Baak *et al.* (2015) contest the occurrence of calcareous nannofossils in Hole 380A, especially at 840.07 mbsf, because they did not record nannofossils in the interval 840–856 mbsf. They write on p. 435: 'The supposed presence of the rare biostratigraphic markers *T. rugosus* and *C. acutus*... should be associated with other taxa constituting the common component of a typical lower Pliocene nannofossil assemblage'. The beginning of this sentence questions our honesty or our expertise, or both, and the end of this sentence implies that we did not record the expected complete nannofossil assemblage.

Our search for nannoplankton was driven by the occurrence of marine dinoflagellate cysts found during a high-resolution study (Popescu, 2006; Fig. 1A). Here, we show in Fig. 1B photographs of the recorded nannofossils. Popescu *et al.* (2010: table 1) published the complete nannoflora, typical of the Lower Pliocene (Fig. 1B1).

In Fig. 1A, we display all the information available for Site 380 between 1019.85 and 645 mbsf, by depth. We chose depth instead of the time plot presented by van Baak *et al.* (2015), because the time plot distorts the curves in a model-driven presentation, the chronology of which is contradicted by our data. Here, the interval 839.30–851.28 mbsf with the high range of surface-water salinity determined by Schrader (1978) agrees with the low percentages of halophytes.

Considering (Fig. 1A):

- the robust data with wide-scale significance, such as the $^{40}Ar/^{39}Ar$ dating at 4.36 ± 0.19 Ma, the N1, N2 and N3 normal palaeomagnetic episodes and the nannofossil markers (*Sphenolithus abies* and *Reticulofenestra pseudoumbilicus* at

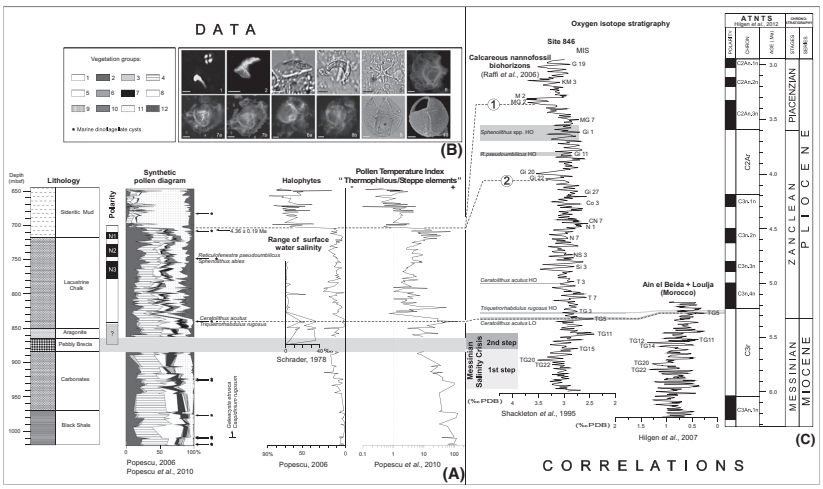

Fig. 1 Chronostratigraphic and environmental data on the lower part of Hole 380A (1019.85–645 mbsf) and proposed correlations. (A) Data presented according to depth. Vegetation groups for the synthetic pollen diagram: 1, tropical elements; 2, subtropical elements; 3, *Cathaya*; 4, warm-temperate elements; 5, *Pinus*; 6, cool-temperate elements; 7, boreal elements; 8, non-significant pollen grains; 9, Mediterranean xerophytes; 10, Cupressaceae; 11, herbs; 12, steppe elements. For details, see Popescu (2006) and Popescu *et al.* (2010). (B) Biostratigraphic markers (scale bar = 10 μm for Figs 1, 6–10; scale bar = 7 μm for Figs 2–5). Calcareous nannofossils: 1, assemblage with *Ceratolithus acutus* and *Reticulofenestra* sp., crossed nicols (840.07 mbsf); 2, *Ceratolithus acutus*, crossed nicols (840.07 mbsf); 3, *Triquetrorhabdulus rugosus*, parallel light (840.07 mbsf); 4, *Amaurolithus primus*, parallel light (840.07 mbsf); 5, *Discoaster brouweri*, parallel light (840.07 mbsf). Dinoflagellate cysts: 6–8, *Galeacysta etrusca* complex (Popescu *et al.*, 2009), fluorescence microscopy: 6, *Spiniferites balcanicus* (846.14 mbsf); 7a,b, *Galeacysta etrusca* (1009.36 mbsf); 8a,b, *Romanodinium areolatum* (1009.36 mbsf); 9,10, *Caspidinium rugosum*, light microscopy and SEM (1009.36 mbsf). (C) Proposed correlations based on consideration of all the proxies. Hypotheses 1 and 2, concerning the upper part of the interval, are discussed in the text. MIS, marine isotope stage; LO, lowest occurrence; HO, highest occurrence.

Correspondence: Dr. Speranta-Maria Popescu, GeoBioStratData.Consulting, 385 Route du Mas Rillier, Rillieux la Pape 69140, France. Tel.: +0682143526; e-mail: speranta.popescu@gmail.com

748.45 mbsf, *Ceratolithus acutus* and *Triquetrorhabdulus rugosus* at 840.07 mbsf), and
- the occurrence of the *Galeacysta etrusca* complex (Popescu *et al*., 2009) and *Caspidinium rugosum* at least from 1009.36 mbsf (FCO at 6.1 Ma),

we consider that the only reliable interpretation is to correlate the interval 864.50–840.00 mbsf with the lowermost Zanclean and, as a consequence, the underlying Pebbly Breccia with the 2nd step of the Messinian Salinity Crisis (Clauzon *et al*., 1996) (Fig. 1C). The normal episodes N1, N2 and N3 can be, respectively, attributed to palaeomagnetic chrons C3n.2n, C3n.3n and C3n.4n, as proposed by van Baak *et al*. (2015) or, allowing for the confidence range of the $^{40}Ar/^{39}Ar$ dating respectively to chrons C3n.1n, C3n.2n and C3n.3n, an interpretation not considered by van Baak *et al*. (2015) (Fig. 1C).

An important change in the pollen record at 703 mbsf, indicating the replacement of forests by open vegetation, has been correlated with the cooling at 3.37 Ma (Fig. 1C), consistent with the record of *Sphenolithus abies* and *Reticulofenestra pseudoumbilicus* at 748.45 mbsf (Popescu *et al*., 2010): the first hypothesis in Fig. 1C. This correlation calls into question the immediately underlying $^{40}Ar/^{39}Ar$ age of 4.36 ± 0.19 Ma and would involve correlating the N1, N2 and N3 normal episodes respectively with chrons C2An.3n, C3n.1n and C3n.2n, a construction that distorts the sedimentation rate (Fig. 1C). As a second hypothesis (Fig. 1C), we can correlate this vegetation change with the cooler MIS Gi22 and Gi20. Accordingly, the N1, N2 and N3 episodes would correspond to chrons C3n.1n, C3n.2n and C3n.3n respectively. Forthcoming studies should close this matter, particularly in achieving magnetostratigraphy of Site 380.

References

van Baak, C.G.C., Radionova, E.P., Golovina, L.A., Raffi, I., Kuiper, K.F., Vasiliev, I. and Krijgsman, W., 2015. Messinian events in the Black Sea. *Terra Nova*, **27**, 433–441.

Clauzon, G., Suc, J.-P., Gautier, F., Berger, A. and Loutre, M.-F., 1996. Alternate interpretation of the Messinian salinity crisis: controversy resolved? *Geology*, **24**(4), 363–366.

Grothe, A., Sangiorgi, F., Mulders, Y.R., Vasiliev, I., Reichart, G.-J., Brinkhuis, H., Stoica, M. and Krijgsman, W., 2014. Black Sea desiccation during the Messinian Salinity Crisis: fact or fiction? *Geology*, **42**, 563–566.

Hilgen, F., Kuiper, K., Krijgsman, W., Snel, E. and van der Laan, E., 2007. Astronomical tuning as the basis for high resolution chronostratigraphy: the intricate history of the Messinian Salinity Crisis. *Stratigraphy*, **4**, 231–238.

Hilgen, F.J., Lourens, L.J. and Van Dam, J.A., 2012. The Neogene Period. In: *The Geological Time Scale 2012* (F. Gradstein, J. Ogg, M. Schmitz and G. Ogg, eds), 1, 29, pp. 923–978. Elsevier, Amsterdam.

Popescu, S.-M., 2006. Late Miocene and early Pliocene environments in the southwestern Black Sea region from high-resolution palynology of DSDP Site 380A (leg 42B). *Palaeogeogr. Palaeoclimatol. Palaeoecol*., **238**, 64–77.

Popescu, S.-M., Dalesme, F., Jouannic, G., Escarguel, G., Head, M.J., Melinte-Dobrinescu, M.C., Sütő-Szentai, M., Bakrac, K., Clauzon, G. and Suc, J.-P., 2009. *Galeacysta etrusca* complex, dinoflagellate cyst marker of Paratethyan influxes into the Mediterranean Sea before and after the peak of the Messinian Salinity Crisis. *Palynology*, **33**, 105–134.

Popescu, S.-M., Biltekin, D., Winter, H., Suc, J.-P., Melinte-Dobrinescu, M.C., Klotz, S., Combourieu-Nebout, N., Rabineau, M., Clauzon, G. and Deaconu, F., 2010. Pliocene and Lower Pleistocene vegetation and climate changes at the European scale: long pollen records and climatostratigraphy. *Quatern. Int*., **219**, 152–167.

Raffi, I., Backman, J., Fornaciari, E., Pälike, H., Rio, D., Lourens, L. and Hilgen, F., 2006. A review of calcareous nannofossil astrobiochronology encompassing the past 25 million years. *Quatern. Sci. Rev*., **25**, 3113–3137.

Schrader, H.-J., 1978. Quaternary through Neogene history of the Black Sea, deduced from the paleoecology of diatoms, silicoflagellates, ebridians, and chrysomonads. In: *Initial Report of the Deep Sea Drilling Project*, Vol. 42, Part 2. (D.A. Ross and Y.P. Neprochnov, eds.), pp. 789–902. U.S. Government Printing Office, Washington.

Shackleton, N.J., Hall, M.A. and Pate, D., 1995. Pliocene stable isotope stratigraphy of Site 846. In: *Proceedings of the Ocean Drilling Program, Scientific Results*, Vol. **138** (N.G. Pisias, L.A. Mayer, T.R. Janecek, A. Palmer-Julson and T.H. van Andel, eds), pp. 337–355. U.S. Government Printing Office, Washington.

Suc, J.-P., Gillet, H., Çağatay, M.N., Popescu, S.-M., Lericolais, G., Armijo, R., Melinte-Dobrinescu, M.C., Şen, Ş., Clauzon, G., Sakınç, M., Zabcı, C., Ucarkus, G., Meyer, B., Çakir, Z., Karakaş, Ç., Jouannic, G. and Macaleţ, R., 2015. The region of the Strandja Sill (North Turkey) and the Messinian events. *Mar. Petrol. Geol*., **66**, 149–164.

Received 4 January 2016; revised version accepted 1 March 2016

